THIS REPORT HAS BEEN DELIMITED

AND CLEARED FOR PUBLIC RELEASE

UNDER DOD DIRECTIVE 5200.20 AND

NO RESTRICTIONS ARE IMPOSED UPON

ITS USE AND DISCLOSURE,

DISTRIBUTION STATEMENT A

APPROVED FOR PUBLIC RELEASE;

DISTRIBUTION UNLIMITED,

Best
Available
Copy

ENSE DOCUMENTATION CENTER

FOR

IENTIFIC AND TECHNICAL INFORMATION

CAMERON STATION, ALEXANDRIA, VIRGINIA

Department of AERONAUTICS and ASTRONAUTICS
STANFORD UNIVERSITY

DDC444808

J. Singer

Creep rupture of ductile materials subjected to strain hardening or time hardening creep

JUNE
1964

SUDAER
NO. 196

Department of Aeronautics and Astronautics
Stanford University
Stanford, California

CREEP RUPTURE OF DUCTILE MATERIALS SUBJECTED TO

STRAIN HARDENING OR TIME HARDENING CREEP

by

Josef Singer[*]
Visiting Associate Professor, Stanford University

SUDAER No.196

June 1964

[*] On leave from the Department of Aeronautical Engineering, Technion,
Israel Institute of Technology, Haifa, Israel

ABSTRACT

An analysis of creep rupture of ductile materials subjected to
strain hardening creep is presented. The analysis is similar to an
earlier one by Hoff, but is based on a different generalization of
the primary creep rate relation. Both approaches are then extended
to time hardening creep. Simple approximate formulae for critical
times are presented and the results of both approaches for the two
types of creep are compared. Correlation with experimental data for
some aluminum-copper, aluminum-magnesium and aluminum-zinc alloys
shows fairly good agreement of rupture times for these very ductile
materials. However, attempted correlation with data for other
materials which do not exhibit such prominent ductility indicates
that the basic assumption of the analysis, that creep rupture is
caused primarily by a process of reduction of area, holds only for
very ductile materials.

TABLE OF CONTENTS

LIST OF ILLUSTRATIONS

NOTATION

A_o initial cross sectional area of specimen

b $(1-p)/p$

m constant in primary creep law, Eq.(1), called sometimes "primary creep index"

p constant in primary creep law, Eq.(1)

R $1 + \epsilon$, defined by Eq.(9)

q $p - 1$

s mp

t time

t_{cr} rupture time

$t_{\epsilon_{nat}}$ rupture time predicted for strain hardening creep with Hoff's generalization

$t_{\epsilon_{ENG}}$ rupture time predicted for strain hardening creep with the alternative generalization proposed here

$t_{TH.\epsilon_{nat}}$ rupture time predicted for time hardening creep with Hoff's generalization

$t_{TH.\epsilon_{ENG}}$ rupture time predicted for time hardening creep with the alternative generalization

t_{exp} rupture time from tests

β $t_{\epsilon_{nat}} / t_{\epsilon_{ENG}}$

γ $t_{TH.\epsilon_{nat}} / t_{TH.\epsilon_{ENG}}$

δ $t_{\epsilon_{nat}} / t_{TH.\epsilon_{nat}}$

ϵ engineering strain

ϵ_{nat} natural strain $= \ln(1+\epsilon)$

η $t_{\epsilon_{ENG}} / t_{TH.\epsilon_{ENG}}$

λ constant in primary creep law, Eq.(1)

NOTATION (Cont'd.)

σ true stress

σ_0 initial applied stress

σ_u ultimate stress of the material at test temperature

INTRODUCTION

The creep rupture of a tensile bar of ductile material, undergoing creep deformations which are governed almost entirely by a steady state creep law, was analyzed by Hoff (Ref.1). A very simple approximate formula was obtained for the critical time, which agreed well with experimental data for pure aluminum and some aluminum alloys. However, many creep curves, especially at higher stresses and temperatures, do not exhibit the usual steady phase, but have a longer primary phase which transforms directly into a tertiary phase (see for example, Fig.1, replotted from Ref.2).

The primary phase is usually considered to be governed by a creep law of the form

$$\epsilon = (\sigma/\lambda)^m \, t^{1/p} \tag{1}$$

where ϵ is the engineering strain, σ the applied stress, t the time and m, λ and p are constants. For variable stress, Eq.(1) has to be considered as defining implicitly the strain rate as a function of the stress and the strain, or as a function of the stress and the time (Ref.3). Then, for strain hardening creep behavior, one obtains

$$\dot{\epsilon} = (1/p)(\sigma/\lambda)^{mp} \, \epsilon^{1-p} \tag{2}$$

which is essentially the relation proposed much earlier by Nadai (Ref.4).

For time hardening behavior, which is sometimes observed when time of exposure has a more pronounced effect than the amount of creep strain, a parallel relation for the primary creep rate results

$$\dot{\epsilon} = (1/p)(\sigma/\lambda)^m \, t^{(1-p)/p} \tag{3}$$

RUPTURE TIME FOR STRAIN HARDENING CREEP

For strain hardening creep, Hoff (Ref.5) obtained the creep rupture time by assuming that Eq.(2) can be generalized to hold for large deformations

$$\dot{\epsilon}_{nat} = (1/p)(\sigma/\lambda)^{mp} \, \epsilon_{nat}^{1-p} \qquad (4)$$

where σ is the true stress and ϵ_{nat} is the natural strain defined by

$$\epsilon_{nat} = \ell n(1+\epsilon) \qquad (5)$$

and

$$\sigma = \sigma_o(1+\epsilon) \qquad (6)$$

σ_o being the initial applied stress

$$\sigma_o = P/A_o \qquad (7)$$

Hoff obtained a very simple approximate formula also for strain hardening creep, which becomes, when p is an integer,

$$t_{cr} \simeq [p/(pm)^p](\lambda/\sigma_o)^{pm} \qquad (8)$$

Hoff's generalization of the primary creep law, Eq.(4), means that the same relation between strain rate, stress and strain is assumed to hold for the entire strain range from primary creep to rupture, provided the relation is expressed in natural strain and strain rate and true stress. In the small strain region, the natural strain practically equals the engineering strains and Eq.(4) reduces to Eq.(2). Hence the assumption implies identical constants in both equations.

However, since primary creep curves are usually given only for small strains, another approach is possible. Instead of the generalization proposed by Hoff, the observed relation between engineering strain rate and strain and stress, Eq.(2), is assumed to hold only for engineering strain rate and strain, but to be valid also in the region

- 2 -

of large strains. The natural strain rate involved in the calculation of rupture time has then to be related appropriately to the engineering strain rate which appears in Eq.(2). It is felt that such an approach gives one more confidence in the use of the primary creep constants which are obtained from experiments at small strains.

In other words, the two approaches are two different extrapolations of Eq.(2) to the region of large strains. The actual applied stress varies, due to the reduction in area, in the same manner in both approaches and is represented by Eq.(6). The extrapolations differ, however, with respect to strain and strain rate.

The analysis is an extension of Hoff's work. As in Refs. 1 and 5, a constant load tensile test is considered, and the material is assumed to be incompressible. The symbol R is also introduced again,

$$R = 1 + \epsilon \tag{9}$$

Hence

$$\epsilon_{nat} = \ln R \tag{10}$$

and

$$\sigma = \sigma_o R \tag{11}$$

For strain hardening creep the strain rate is governed by Eq.(2), ϵ being the creep strain (the total strain less the initial elastic and plastic strain). Rupture occurs at large strains, and hence the natural strain rate is required for calculation of the time to rupture. Now, Eq.(5) may be rewritten, on account of Eq.(9),

$$e^{\epsilon_{nat}} = 1 + \epsilon = R \tag{12}$$

or

$$\epsilon = e^{\epsilon_{nat}} - 1 = R - 1 \tag{13}$$

- 3 -

By differentiating Eq. (5) with respect to time, one obtains

$$\dot{\epsilon}_{nat} = \left[1/(1+\epsilon)\right]\dot{\epsilon} \tag{14}$$

Substitution of $\dot{\epsilon}$ from Eq. (2), ϵ from Eq. (13) and σ from Eq. (11) into Eq. (14) yields

$$d\epsilon_{nat}\, dt = (1/p)(\sigma_o R/\lambda)^{m} \left[(R-1)^{1-p}/R\right] \tag{15}$$

For convenience let

$$q = p - 1 \tag{16}$$
$$\text{and} \quad s = mp$$

Separation of variables of Eq. (15) and integration yield the critical time

$$t_{cr} = p(\lambda/\sigma_o)^s \int_1^{(\sigma_u/\sigma_o)} \left[(R-1)^q/R^s\right] dR \tag{17}$$

where σ_u is the ultimate stress of the material at the test temperature.

For most materials, p may be approximated by 2 or 3. For these values the critical time is given by

$$t_{cr} = 2(\lambda/\sigma_o)^s \left\{ -\left[1/(2-s)\right]\left[1 - (\sigma_o/\sigma_u)^{s-2}\right] + \left[1/(1-s)\right]\left[1 - (\sigma_o/\sigma_u)^{s-1}\right] \right\} \tag{18}$$

for $q = 1$ $(p = 2)$

or

$$t_{cr} = 3(\lambda/\sigma_o)^s \left\{ -\left[1/(3-s)\right]\left[1 - (\sigma_o/\sigma_u)^{s-3}\right] + \left[2/(2-s)\right]\left[1 - (\sigma_o/\sigma_u)^{s-2}\right] \right.$$
$$\left. -\left[1/(1-s)\right]\left[1 - (\sigma_o/\sigma_u)^{s-1}\right] \right\} \tag{19}$$

for $q = 2$ $(p = 3)$.

- 4 -

For other values of q Eq.(17) can be integrated in a similar manner to yield similar expressions for t_{cr} . Now, since s is generally fairly large, $(c_o/\sigma_u)^{s-3}$ and the corresponding higher powers of (σ_o/σ_u) in Eqs.(18) and (19) may be neglected in comparison to unity, even when σ_o is not far from σ_u . Eqs.(18) and (19) may therefore be simplified to

$$t_{cr} \simeq (\lambda/\sigma_o)^s \left[2/(s-2)(s-1) \right] \qquad \text{for} \quad p = 2 \qquad (20)$$

and

$$t_{cr} \simeq (\lambda/\sigma_o)^s \left[6/(s-3)(s-2)(s-1) \right] \qquad \text{for} \quad p = 3 \qquad (21)$$

- 5 -

The analysis can readily be extended to time hardening creep defined by the creep law of Eq.(3), by both approaches. First, generalization of Eq.(3) in the manner proposed by Hoff for strain hardening creep yields for the natural strain rate

$$\hat{\epsilon}_{nat} = (1/p)(\sigma/\lambda)^m t^{(1-p)/p} \tag{22}$$

With the quantities defined by Eqs.(9), (10), (11) and (16) and denoting

$$(1-p)/p = b \tag{23}$$

one can rewrite Eq.(22) as

$$d\ell nR/dt = (1/p)(\sigma_0 R/\lambda)^m t^b \tag{24}$$

Separation of variables and integration yields

$$
\begin{aligned}
t_{cr} &= \left\{ \left[(b+1)p/m \right] (\lambda/\sigma_0)^m \left[1 - (\sigma_0/\sigma_u)^m \right] \right\}^{1/(b+1)} \\
&= (1/m)^p (\lambda/\sigma_0)^s \left[1 - (\sigma_0/\sigma_u)^m \right]^p
\end{aligned} \tag{25}
$$

since

$$b + 1 = 1/p \tag{26}$$

Now, if $\sigma_u \gg \sigma_0$

$$\left[1 - (\sigma_0/\sigma_u)^m \right]^p \approx 1 - p(\sigma_0/\sigma_u)^m \approx 1 \tag{27}$$

provided m is sufficiently large. As p can be taken 2 or 3 for most materials and m is usually larger than 3, the approximation of Eq.(27) does, in general, not involve large errors. With this approximation Eq.(25) becomes

$$t_{cr} \approx (1/m^p)(\lambda/\sigma_0)^s \tag{28}$$

- 6 -

However, it should be noted that the approximation here is inferior to that employed in the case of strain hardening creep. There, at most $(\sigma_o/\sigma_u)^{pm-3}$ was neglected in comparison with unity, whereas in Eq.(27) $p(\sigma_o/\sigma_u)^m$ is neglected in comparison with unity. Hence the error implied by Eq.(28) is $p(\sigma_u/\sigma_o)^{mp-m-3}$ times as large as that introduced by the approximation leading to Eqs.(8) or (20) and (21).

In the second approach, Eq.(3) is again assumed to hold for the engineering strain rate for both small and large strains. With the quantities defined by Eqs.(9), (10), (11), (16) and (23) and with Eqs.(3) and (14), the natural strain rate can be rewritten as

$$d\epsilon_{nat}/dt = (1/pR)(\sigma_o R/\lambda)^m t^b \qquad (29)$$

Separation of variables and integration yields then, on account of Eq.(26),

$$t_{cr} = \left[1/(m-1)\right]^p (\lambda/\sigma_o)^s \left[1 - (\sigma_o/\sigma_u)^{m-1}\right]^p \qquad (30)$$

For $\sigma_u \gg \sigma_o$, an approximate expression can again be obtained for the critical time provided m is sufficiently large,

$$t_{cr} \simeq \left[1/(m-1)^p\right](\lambda/\sigma_o)^s \qquad (31)$$

The accuracy of this approximation is, however, even lower than that of Eq.(28), since here $p(\sigma_o/\sigma_u)^{m-1}$ is neglected in comparison with unity. The error introduced by Eq.(31) relative to Eq.(30) is therefore (σ_u/σ_o) times that introduced in Eq.(28).

COMPARISON OF RUPTURE TIMES

It is of interest to compare the rupture times obtained by the various approaches. If one compares the approximate formulae for the critical times, very simple relations are obtained. However, as the approximations in these formulae are different, the more exact formulae for the rupture time have to be employed in the comparison for the low values of m , when the initial applied stress approaches the ultimate stress and the approximations lose their validity. Only the simple approximate relations are given below, but the results of computations with the more exact relations are also shown in Figs. 2 and 3.

If β denotes the relation of the rupture time for strain harden-ing obtained by Hoff to that obtained by the alternative generalization proposed in this paper,

$$\beta = (s-1)(s-2)/s^2 \qquad \text{for} \quad p = 2 \qquad (32)$$

and

$$\beta = (s-1)(s-2)(s-3)/s^3 \qquad \text{for} \quad p = 3 \qquad (33)$$

if the approximate formulae, Eqs.(8) and (20), (21) are compared. Fig. 2 shows a plot of β versus the primary creep index m . For two typical initial applied stress to ultimate stress ratios, (σ_o/σ_u) = 0.5 and (σ_o/σ_u) = 0.9 , the values of β as obtained from a com-parison of the more exact Eq.[59] of Ref.5 and Eqs.(18) and (19) are also shown.

If one compares the results of the two approaches for time harden-ing creep, the approximate formulae Eqs.(28) and (31) are related by

$$\gamma = \left[(m-1)/m\right]^p \qquad (34)$$

This ratio is plotted in Fig. 3 for p = 2 and p = 3 . The relation of the more exact formulae Eqs.(25) and (30) is also included for (σ_o/σ_u) = 0.5 and (σ_o/σ_u) = 0.9 .

Figures 2 and 3 show that as the primary creep index m increases, the difference between the two approaches diminishes both for strain hardening and time hardening creep. For low applied stresses, say, $\sigma_o \leq 0.5\,\sigma_u$, the noticeable difference between the two approaches, predicted by the approximate relations, is verified by the results obtained by the more exact relations. When the applied stress approaches the ultimate stress, for example, when $\sigma_o = 0.9\,\sigma_u$, the difference practically disappears. This would be expected since the strains at rupture tend to be small when the applied stress approaches the ultimate.

Similar simple relations can be obtained by comparison of the approximate rupture time for strain hardening creep with that for time hardening creep by one of the approaches. For the first approach, which assumes that the primary creep relations hold for the entire strain range if expressed in natural strain rates and strains, the rupture time for strain hardening creep divided by that for time hardening creep yields

$$\delta = p!/p^p \tag{35}$$

For the second approach, which assumes the primary creep relations to hold only for engineering strain rates and strains, but to be valid also in regions of large strains, the rupture time for strain hardening creep divided by that for time hardening creep yields

$$\eta = (m-1)/(2m-1) \qquad \text{for } p = 2 \tag{36}$$

and

$$\eta = 2(m-1)^2/(3m-2)(3m-1) \qquad \text{for } p = 3 \tag{37}$$

However, these relations, Eqs. (35), (36) and (37), are again valid only within the accuracy of the approximations, on account of the considerable difference in the error included in the approximate formulae.

The comparison shows that the second approach yields longer critical times than the first one, in both types of creep deformation. Also time hardening creep will yield longer rupture times than strain

- 9 -

hardening creep by both approaches. However, since the analysis is basically a generalization of empirical primary creep laws, only correlation with experimental data can determine the relative usefulness of the proposed formulae. This is attempted in the next section.

CORRELATION WITH EXPERIMENTAL DATA AND DISCUSSION

The results of tests carried out by Robinson, Tietz and Dorn
(Ref.2) were compared with the theoretical predictions by the two
approaches for strain hardening and time hardening creep. The test
materials were a series of high purity binary alpha solid solutions
in aluminum. Three groups of aluminum alloys were compared: copper-
aluminum alloys, magnesium-aluminum alloys and zinc-aluminum alloys.
Each group includes four alloys with different percentages of alloying
element, and all tests were at $300^{\circ}F$. In Tables 1, 2 and 3 the pre-
dicted and experimental values of the rupture times are given for dif-
ferent applied stresses. The data for the magnesium-aluminum alloys
are also plotted in Fig.4.

To obtain a theoretical rupture time, the primary creep constants
p, m and λ have first to be found from the creep curves of Ref.2.
The left hand portions of the creep curves (for relatively short times)
have to be used to find these constants, since for longer times the
curves include the effects of the reduction in area. The time index
p is found from Eq.(1) with σ and λ constant. For the alloys of
Figs. 4-6 of Ref.2, the nearest integer for p is 2. Now, from
short time stress-strain curves at $300^{\circ}F$, Figs.15-17 of Ref.2, the
initial strains are found for the nominal applied stresses. The total
strain less the initial strain is the creep strain. The creep strains
at particular times are plotted versus the corrected applied stress
on a log-log scale yielding straight lines whose slope is m. The
integer nearest to the average value of m obtained from about 5 or
6 of such isochronous lines is taken as the appropriate value. λ is
then found from Eq.(1) with these p and m from about 10 points and
averaged.

In Tables 1, 2 and 3, the rupture time for strain hardening creep
with Hoff's generalization is denoted $t_{\varepsilon_{nat}}$, and that obtained with
the alternative generalization of this paper $t_{\varepsilon_{ENG}}$. The rupture
times for time hardening creep are similarly denoted $t_{TH.\varepsilon_{nat}}$ and $t_{TH.\varepsilon_{ENG}}$,

- 11 -

respectively. The more exact formulae, Eqs.(18), (25) and (30), and an expression which is equivalent to Eq.(59) of Ref.5, have been used in the calculation of the rupture times.

Fairly good agreement is found for most of the tests. The rupture times for time-hardening creep, with the generalization of the primary creep law proposed in this paper, appear to be closest to the experimental results. Better agreement is found for the magnesium-aluminium and copper-aluminum alloys (except the 0.101% Cu alloy for which the predictions are noticeably too long)than for the zinc-aluminum alloys. It is interesting to note that the rupture times computed with the assumption of strain-hardening creep are rather conservative for all the test results (except those for two tests of 0.101% Cu Al alloy). It might be added, that if the plastic strain component is taken into account (Ref.6) the predicted rupture time is further shortened. Since this effect would be most noticeable at the high applied stresses, where the predictions based on time-hardening creep often exceed the experimental rupture times, it would tend to improve the overall agreement of the time-hardening theory. It appears, therefore, that for the materials compared here, a time-hardening creep law provides a realistic description of the rupture behavior.

An extensive literature search for additional experimental data of primary creep and rupture for ductile materials revealed a remarkable scarcity of such data. Most investigators report either details of primary creep behavior or rupture times, but very seldom both. Since only creep curves which do not exhibit a significant steady phase are suitable for comparison with the present theory, no additional data was found. However, through the courtesy of the Research Division of High Duty Alloys Ltd., Slough, England, creep curves for RR 58 and RR 257 aluminium alloys (which are used in the Anglo-French supersonic transport) were obtained with records of rupture times and corresponding total strains (Ref.7). Some of these curves had no significant secondary phase. Correlation was attempted with some of these curves, but the predicted rupture times greatly exceeded the experimental values (the computed values were 50 to 30,000 times the experimental ones). As a

check on the order of magnitude of the prediction, the rupture times were computed by the steady creep analysis of Ref.1 (the steady creep constants were obtained from approximate tangents to the central portion of the creep curves). However, again the predictions were many times too large, though to a lesser extent (6 to 60 times).

During the literature search some creep curves of suitable form were encountered, for which rupture times were also reported. However, they represented materials which exhibited only small amounts of permanent deformation prior to fracture, and hence cannot be adequately described by the present theory. For comparison, correlation was attempted for a typical case of this group, a 5% molybdenum steel at $1020^\circ F$ (Ref.8). The predicted rupture times greatly exceeded the experimental values (by 400 to 500,000 times), and a steady creep analysis produced similar discrepancies (700 to 3000 times).

It may be pointed out that "ductile theory", which assumes rupture by reduction of area, disagrees noticeably with experiments also for creep with a predominant secondary phase in the case of age-hardening aluminium alloys. For example, for 7075 TC at $375^\circ F$ (Ref.5) rupture times 10 to 20 times the experimental ones are predicted.

Hence it is apparent that theories which are based on the premise that rupture is caused primarily .y a necking process are applicable to very ductile materials only (like those tested in Ref.2 or the 3003 and 5052 aluminium alloys tested in Ref.9). For other materials one has to turn to other theories which try to account for brittle or partly brittle behavior at rupture (see, for example, Refs.10, 11 or 12).

It may be observed, that the difference between the rupture times obtained from four different creep laws, is insignificant compared to the difference between predicted and experimental values, except for the very ductile materials of Ref.2. Hence, the marked disagreement between theory and experiment for the more commonly used alloys cannot be attributed to inadequacies in the creep laws, but rather to the character of the rupture process.

- 13 -

ACKNOWLEDGMENT

The author would like to express his gratitude to Professor N. J. Hoff and to Dr. R. L. Carlson of Stanford University for helpful discussions.

REFERENCES

1. N. J. Hoff, The Necking and the Rupture of Rods Subjected to Constant Tensile Loads. Journal of Applied Mechanics, Vol.20, No.1, p.105, March 1953.

2. A. T. Robinson, T. E. Tietz and J. E. Dorn, The Functions of Alloying Elements in the Creep Resistance of Alpha Solid Solutions of Aluminum, Transactions of American Society for Metals, Vol.44, p.896, 1952.

3. N. J. Hoff, Stress Distribution in the Presence of Creep, Chapter 12 of High Temperature Effects in Aircraft Structures, edited by N. J. Hoff. Pergamon Press, p.248, London, 1958.

4. A. Nadai, The Influence of Time Upon Creep, S. Timoshenko 60th Anniversary Volume, The Macmillan Co., New York, 1938, p.155.

5. N. J. Hoff, Structures and Materials for Finite Lifetime, Proceedings of the First International Congress of the Aeronautical Sciences, Advances in Aeronautical Sciences, Vol.2, Pergamon Press, p.928, London, 1959.

6. R. L. Carlson, An Analysis of Creep Rupture, SUDAER Report No.183, Stanford University, February 1964.

7. Private Communications from W. M. Doyle, Research Division, High Duty Alloys Ltd., Slough, England, February and March 1964.

8. A. E. Johnson and N. E. Frost, Note on the Fracture Under Complex Stress Creep Conditions of a 5% Molybdenum Steel at 550°C and a Commercially Pure Copper at 250°C, Creep and Fracture of Metals at High Temperatures, Proceedings of Symposium held at NPL 1954, p.363, HMSO, London, 1956.

9. J. E. Dorn and T. E. Tietz, Creep and Stress-Rupture Investigations on Some Aluminum Alloy Sheet Metals, Proceedings of the American Society for Testing Materials, Vol.49, 1949, p.815.

10. C. Crussard and T. Friedel, Theory of Accelerated Creep and Rupture, Creep and Fracture of Metals at High Temperatures, Proceedings of Symposium held at NPL 1954, p.243, HMSO, London, 1956.

11. L. M. Kachanov, Rupture Time Under Creep Conditions, Problems of Continuum Mechanics, Noordhoff, Groningen, 1961, p.202.

12. F. K. G. Odqvist, On Theories of Creep Rupture, Proceedings of the IUTAM Symposium on Second Order Effects in Elasticity, Plasticity and Fluid Dynamics, Haifa, Israel, April 1962.
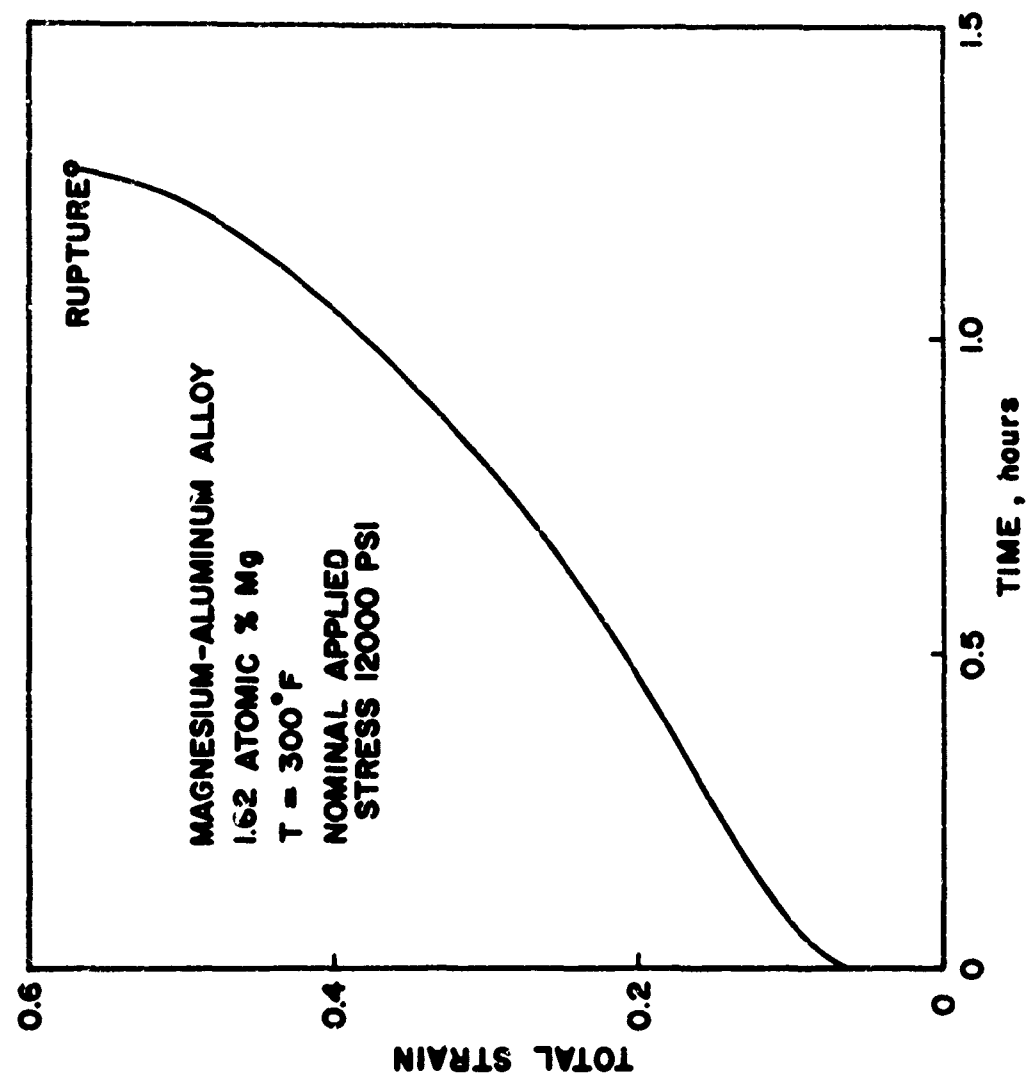
- 15 -

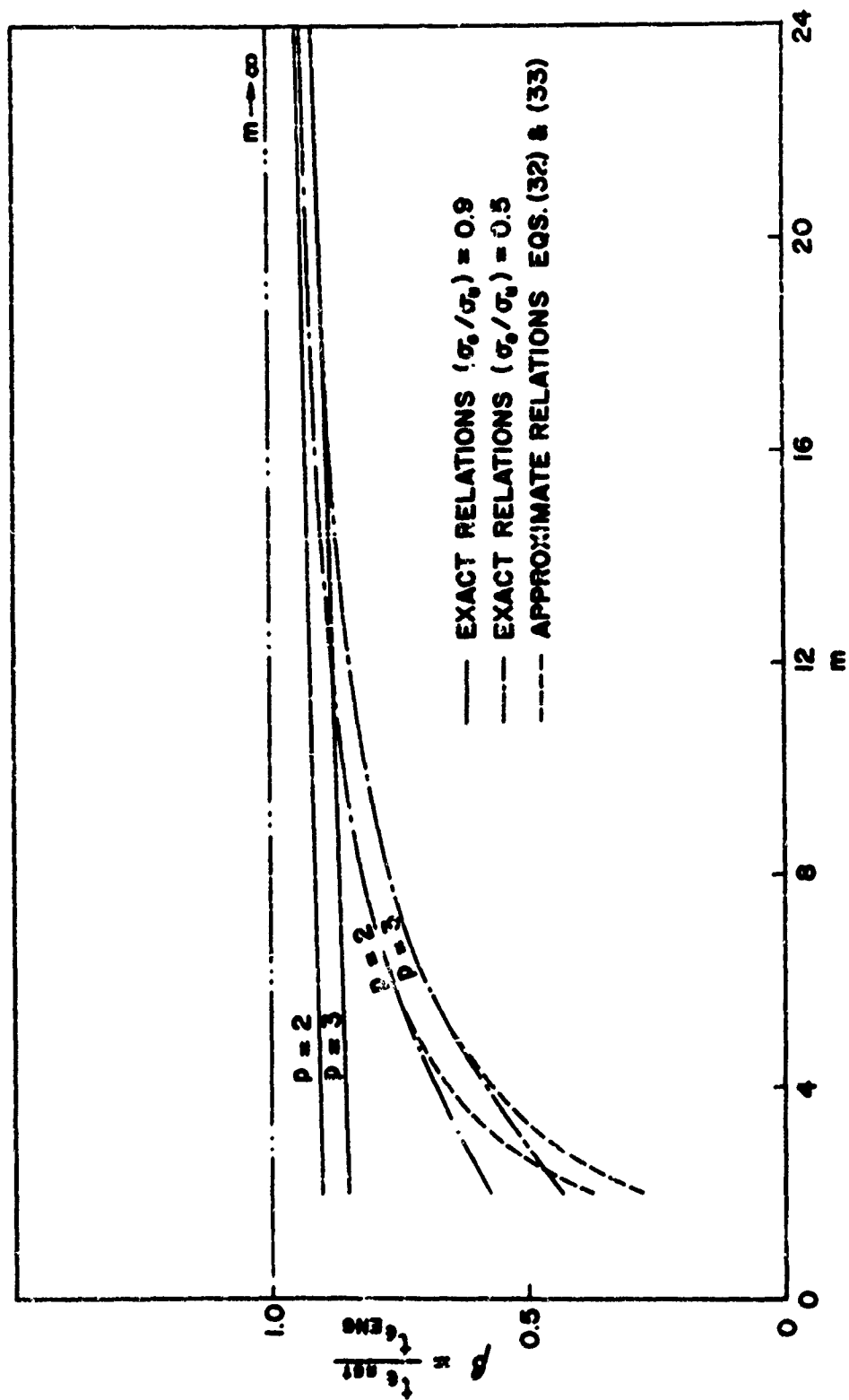FIG. 1. TYPICAL CREEP CURVE WITHOUT SECONDARY CREEP
(replotted from Ref.2)

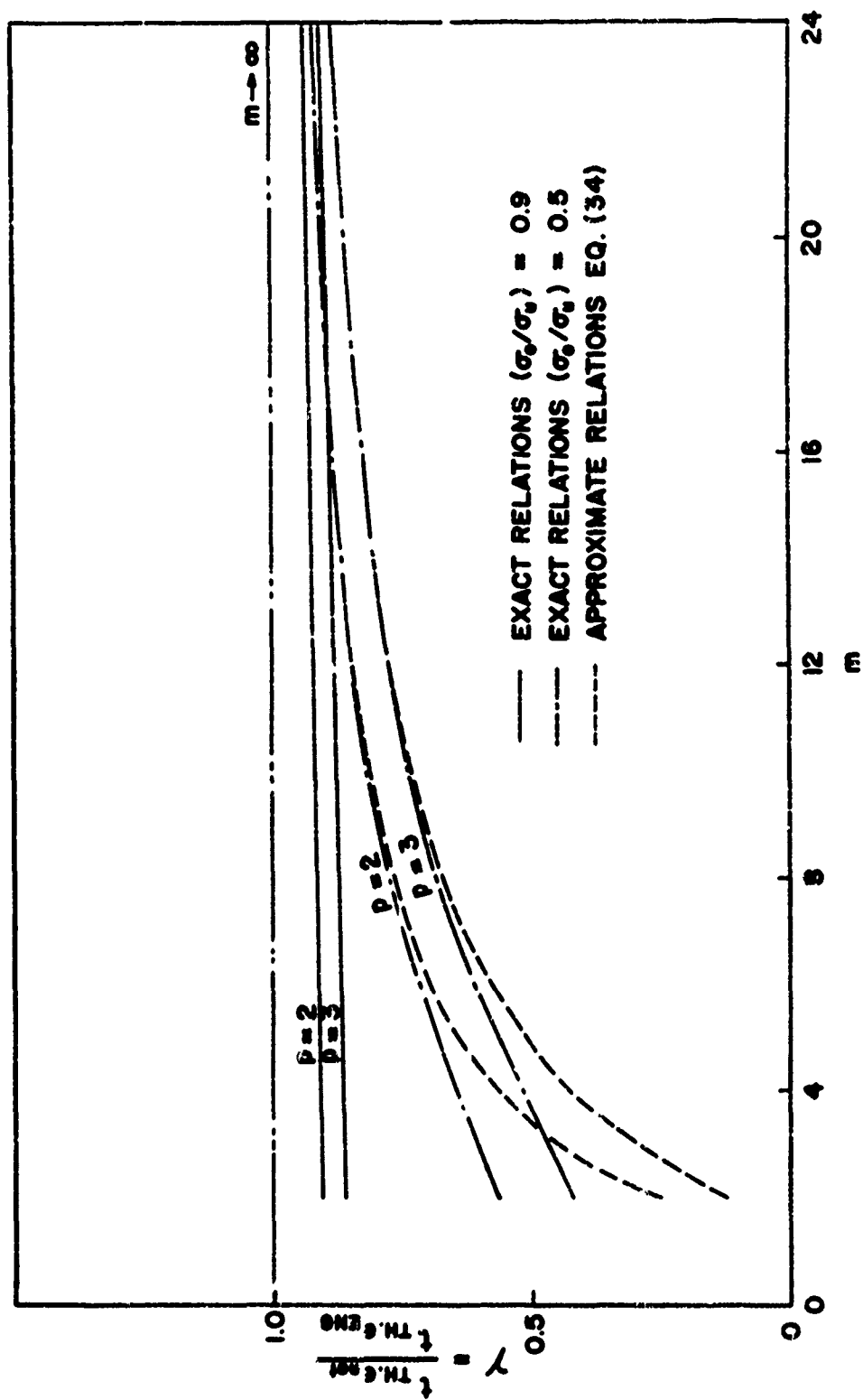FIG. 2. COMPARISON OF RUPTURE TIMES FOR STRAIN HARDENING CREEP

17

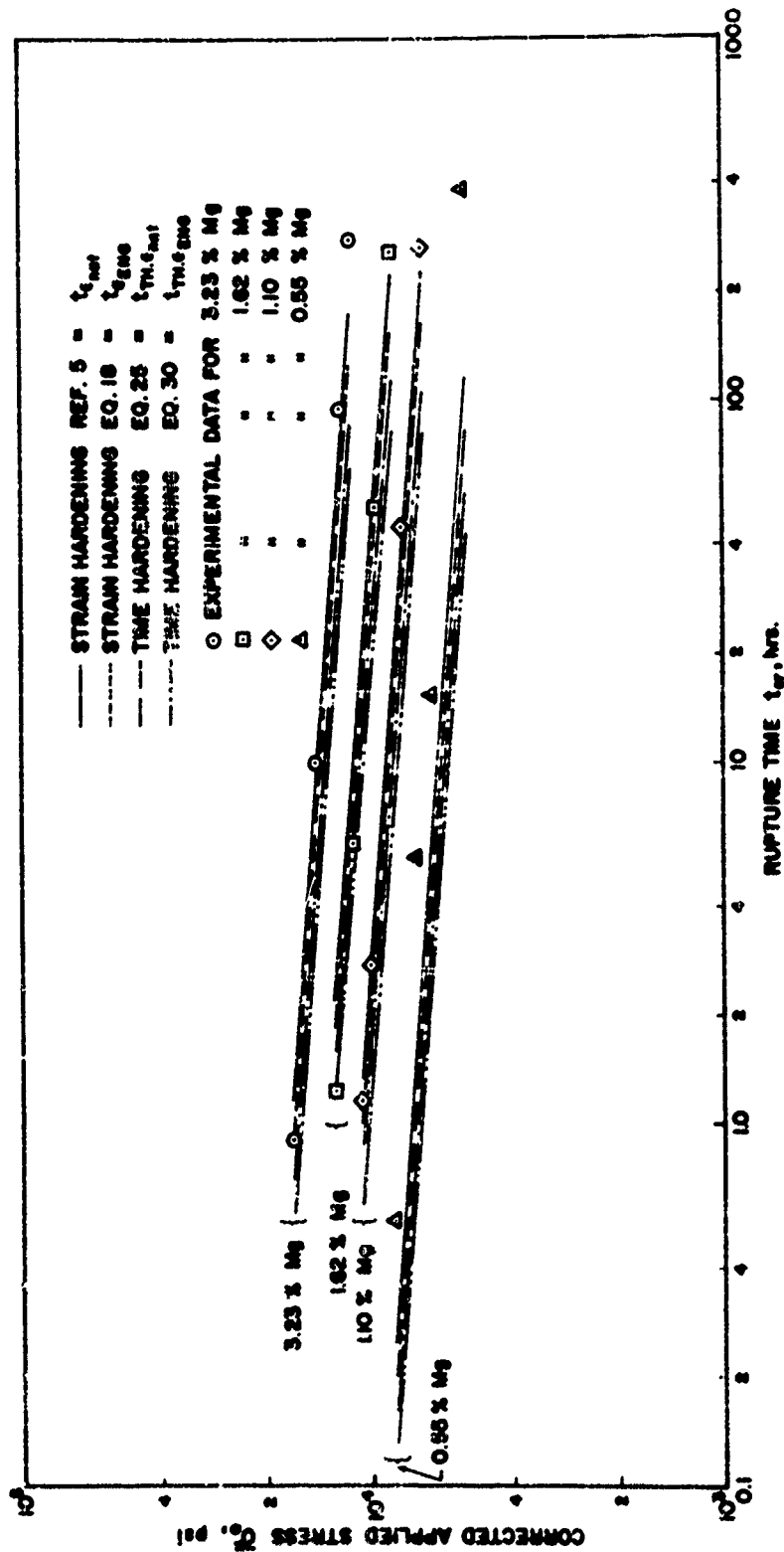FIG. 3. COMPARISON OF RUPTURE TIMES FOR TIME HARDENING CREEP

18

FIG. 4. COMPARISON OF THEORY WITH TESTS ON ALUMINUM
MAGNESIUM ALLOYS BY ROBINSON, TIETZ and DORN
(Ref.2)

19

TABLE 1

Comparison of Theory and Experiment: Copper-Aluminum
Alloys at 300°F Tested by Robinson, Tietz and Dorn

Atomic % of Alloying Element	Nominal Appl.Stress (psi)	Predicted Rupture Times (Hours)				Experimental Rupture Times (Ref.2) $t_{exp.}$
		Strain Hardening (Ref.5)		Time Hardening		
		$t_{\epsilon_{nat}}$	$t_{\epsilon_{ENG}}$	$t_{TH.\epsilon_{nat}}$	$t_{TH.\epsilon_{ENG}}$	
0.029% Cu	2800	29.7	50.9	54.7	102	154
	3500	6.71	10.9	11.5	19.7	26.4
	4000	2.56	4.12	4.12	6.56	6.73
	4800	0.48	0.66	0.67	0.93	1.00
0.054% Cu	2900	61.1	92.7	119	201	216
	3500	12.6	18.9	23.9	38.9	49.4
	4000	4.01	5.94	7.37	11.6	13.0
	5000	0.51	0.71	0.83	1.19	2.12
0.101% Cu	3000	501	696	995	1533	380
	3500	104	144	205	312	100
	4000	25.8	36.3	51.1	76.6	38.0
	6000	0.27	0.35	0.44	C.59	1.01
0.233% Cu	4000	634	881	1257	1929	>1000
	4800	96.0	156	191	289	220
	5500	23.7	32.6	45.3	67.0	41.0
	6500	3.86	4.06	7.03	9.95	7.60
	7500	0.70	0.93	1.18	1.57	1.28

TABLE 2

Comparison of Theory and Experiment: Magnesium-Aluminum
Alloys at 300°F Tested by Robinson, Tietz and Dorn

Atomic % of Alloying Element	Nominal Appl.Stress (psi)	Predicted Rupture Times (Hours)				Experimental Rupture Times $t_{exp.}$ (Ref.2)
		Strain Hardening		Time Hardening		
		$t_{\varepsilon_{rat}}$ (Ref.5)	$t_{\varepsilon_{ENG}}$	$t_{TH \cdot \varepsilon_{rat}}$	$t_{TH \cdot \varepsilon_{ENG}}$	
0.55% Mg	5300	42.4	55.5	32.6	116	385
	6500	3.17	4.08	5.84	7.87	15.5
	7200	0.73	0.93	1.27	1.64	5.44
	8000	0.13	0.16	0.20	0.24	0.54
1.10% Mg	7000	82.0	107	163	234	266
	8000	14.6	19.1	28.7	40.7	45.0
	9500	1.40	1.82	2.50	3.44	2.78
	10000	0.60	0.78	0.99	1.33	1.16
1.62% Mg	8500	82.0	112	154	224	260
	9400	28.1	38.2	50.8	71.8	50.8
	10800	5.87	7.65	9.71	13.0	6.00
	12000	1.31	1.61	1.92	2.38	1.23
3.23% Mg	11300	65.0	85.0	126	177	280
	12000	29.7	38.7	57.2	79.1	95.4
	14000	3.82	4.93	7.04	9.38	10.1
	16000	0.57	0.70	0.92	1.16	0.91

TABLE 3

Comparison of Theory and Experiment: Zinc-Aluminum
Alloys at 300°F Tested by Robinson, Tietz and Dorn

| Atomic % of Alloying Element | Nominal Appl.Stress (psi) | Predicted Rupture Times (Hours) | | | | Experimental Rupture Times (Ref.2) $t_{exp.}$ |
| | | Strain Hardening (Ref.5) | | Time Hardening | | |
		$t_{\epsilon_{nat}}$	$t_{\epsilon_{ENG}}$	$t_{TH.\epsilon_{nat}}$	$t_{TH.\epsilon_{ENG}}$	
0.21% Zn	2500	28.3	42.3	54.3	89.7	268
	3000	5.86	8.69	10.8	17.1	36.3
	3400	1.87	2.70	3.28	4.97	8.00
	4000	0.33	0.44	0.51	0.71	0.31
0.40% Zn	2500	22.7	35.7	43.6	72.0	200
	3000	4.62	6.63	8.68	13.7	25.6
	3400	1.49	2.13	2.63	3.97	6.77
	4000	0.26	0.35	0.41	0.56	1.20
0.76% Zn	2500	25.9	39.2	49.9	82.7	206
	2800	9.81	14.7	18.5	29.9	42.2
	3400	1.82	2.64	3.22	4.89	8.00
	4000	0.33	0.45	0.53	0.74	1.29
1.62% Zn	2300	70.9	98.4	141	217	339
	2500	30.5	42.3	60.3	92.3	155
	2800	9.63	13.4	18.9	28.7	50.2
	3400	1.22	1.69	2.34	3.44	8.00
	4000	0.20	0.27	0.37	0.52	1.70

Chief of Naval Research
Department of the Navy (2)
Washington 25, D. C.
Attn: Code 430

Commanding Officer
Office of Naval Research (1)
Branch Office
495 Summer Street
Boston 10, Massachusetts

Commanding Officer
Office of Naval Research (1)
Branch Office
John Crerar Library Building
86 E. Randolph Street
Chicago 11, Illinois

Commanding Officer
Office of Naval Research (1)
Branch Office
346 Broadway
New York 13, New York

Commanding Officer
Office of Naval Research (1)
Branch Office
1030 E. Green Street
Pasadena, California

Commanding Officer
Office of Naval Research (1)
Branch Office
1000 Geary Street
San Francisco, California

Commanding Officer
Office of Naval Research (25)
Branch Office
Navy No. 100, Fleet Post Office

Director
Naval Research Laboratory
Washington 25, D. C.
Attn: Tech. Info. Officer (6)
       Code 6200 (1)
       Code 6205 (1)
       Code 6250 (1)
       Code 6260 (2)

Armed Services Technical Information
Agency (10)
Arlington Hall Station
Arlington 12, Virginia

Office of Technical Services
Department of Commerce (1)
Washington 25, D. C.

Director of Defense Research and Engineering
The Pentagon (1)
Washington 25, D. C.
Attn: Technical Library

Chief, Defense Atomic Support Agency
The Pentagon
Washington 25, D. C.
Attn: Technical Information Division (2)
       Weapons Effects Division (1)
       Special Field Projects (1)
       Blast and Shock Branch (1)

Office of the Secretary of the Army
The Pentagon (1)
Washington 25, D. C.
Attn: Army Library

Chief of Staff
Department of the Army
Washington 25. D. C.
Attn: Development Branch (R and D Div.) (1)
       Research Branch (R and D Div. (1)
       Special Weapons Br (R and D Div. (1)

Office of the Chief of Engineers
Department of the Army
Washington 25, D. C.
Attn: ENG-ML Lib. Br., Adm. Ser. Div. (1)
       ENG-WD Planning Div. Civ 1 Wks. (1)
       ENG-EB Port. Constr. Br., Eng.
              Div., Mil. Constr. (1)
       ENG-EA Struc. Br., Eng. Div.,
              Mil. Constr. (1)
       ENG-NB Special Engr. Br., Eng.
              R and D Div. (1)

Commanding Officer
Engineer Research Development Laboratory (2)
Fort Belvoir, Virginia

Office of the Chief of Ordnance
Department of the Army
Washington 25, D. C.
Attn. Research and Materials
      Branch (Ord R and D Div.) (1)

Office of the Chief Signal Officer
Department of the Army
Washington 25, D. C.
Attn: Engineering and Technical Division (1)

Commanding Officer
Watertown Arsenal (1)
Watertown, Massachusetts
Attn: Laboratory Division

Office of Ordnance Research
2127 Myrtle Drive
Duke Station
Durham, North Carolina
Attn: Division of Engineering Sciences (4)

Commanding Officer
Squier Signal Laboratory
Fort Monmouth, New Jersey
Attn: Components and Materials Branch (1)

Chief of Naval Operations
Department of the Navy
Washington 25, D. C.
Attn: Op 91 (1)
      Op 03EG (2)

Commandant, Marine Corps
Headquarters, U. S. Marine Corps (1)
Washington 25, D. C.

Commander
Wright Air Development Center
Wright-Patterson Air Force Base
Dayton, Ohio
Attn: Dynamics Branch (1)
      Aircraft Laboratory (1)
      WCLSY (1)

Commanding Officer
USNOEU
Kirtland Air Force Base
Albuquerque, New Mexico
Attn: Code 20 (Dr. J. N. Brennan) (1)

Chief, Bureau of Ships
Department of the Navy
Washington 25, D. C.
Attn: Code 106 (1)
      Code 335 (1)
      Code 345 (1)
      Code 366 (1)
      Code 420 (1)
      Code 421 (1)
      Code 423 (2)
      Code 425 (1)
      Code 440 (1)
      Code 442 (2)
      Code 443 (1)
      Code 1500 (1)

Chief, Bureau of Naval Weapons
Department of the Navy
Washington 25 D. C.
Attn RRMA (1)
      RAAV-14 (1)
      RAAD (1)
      RAAD-2 (1)
      RRBV-7 (1)
      RRB-6 (1)
      RRRH (1)
      DLI-3 (1)
      R (1)
      RM (1)
      RV (1)
      RMLG (1)
      RMGA (1)
      RR (1)

Commanding Officer
Frankford Arsenal
Bridesburg Station
Philadelphia 37, Pennsylvania
Attn: Laboratory Division (1)

Special Projects Office
Bureau of Naval Weapons
Department of the Navy
Washington 25, D. C.
Attn: Missile Branch (2)
      Technical Director (1)

Chief, Bureau of Yards and Docks
Department of the Navy
Washington 25, D. C.
Attn: Code D-202 (1)
      Code D-202.3 (1)
      Code D-220 (1)
      Code D-222 (1)
      Code D-410C (1)
      Code D-440 (1)
      Code D-500 (1)

Commanding Officer and Director
David Taylor Model Basin
Washington 7, D. C.
Attn: Code 140 (1)
      Code 600 (1)
      Code 700 (1)
      Code 720 (1)
      Code 725 (1)
      Code 731 (1)
      Code 740 (2)

Commander
U.S. Naval Ordnance Laboratory
White Oak, Maryland
Attn: Technical Library (2)
      DE (1)
      DF (1)
      K (1)

Director
Materials Laboratory (1)
New York Naval Shipyard
Brooklyn 1, New York

Commander
Portsmouth Naval Shipyard (2)
Portsmouth New Hampshire

Commander
Mare Island Naval Shipyard (2)
Vallejo, California

Commanding Officer and Director
U.S. Naval Electronics Laboratory (1)
San Diego 52, California

Officer-in-Charge
Naval Civil Engineering Research (2)
and Evaluation Laboratory
U.S. Naval Construction Battalion Center
Port Hueneme, California

Director
Naval Air Experiment Station
Naval Air Material Center
Naval Base
Philadelphia 12, Pennsylvania
Attn: Materials Laboratory (1)
      Structures Laboratory (1)

Officer-in-Charge
Underwater Explosion Research Division (2)
Norfolk Naval Shipyard
Portsmouth, Virginia
Attn: Dr. N. M. Schauer

Commander
U.S. Naval Proving Ground (1)
Dahlgren, Virginia

Supervisor of Shipbuilding, USN and
Naval Inspector of Ordnance (1)
General Dynamics Corporation
Electric Boat Division
Groton, Connecticut

Supervisor of Shipbuilding, USN and
Naval Inspector of Ordnance (1)
Newport News Shipbuilding and Dry Dock Co
Newport News, Virginia

Supervisor of Shipbuilding, USN and
Naval Inspector of Ordnance (1)
Ingalls Shipbuilding Corporation
Pascagoula, Mississippi

Commanding Officer
U.S. Naval Administrative Unit (1)
Massachusetts Institute of Technology
Cambridge 39, Massachusetts

Officer-in-Charge
Postgraduate School for Naval Officers (1)
Webb Institute of Naval Architecture
Crescent Beach Road
Glen Cove, Long Island, New York

Superintendent
Naval Weapons Plant (1)
Washington 25, D. C.

Commander
Naval Ordnance Test Station
China Lake, California
Attn: Physics Division (1)
        Mechanics Division (1)

Commanding Officer
Naval Ordnance Test Station (1)
Underwater Ordnance Division
3202 E. Foothill Boulevard
Pasadena 8, California
Attn: Structures Division

Commanding Officer and Director
U.S. Naval Engineering Experiment Station
Annapolis, Maryland (1)

Superintendent
U.S. Naval Postgraduate School (2)
Monterey, California

Commandant
Marine Corps Schools
Quantico, Virginia
Attn: Director, Marine Corps Development (1)
        Center

Commanding General
U.S. Air Force
Washington 25, D. C.
Attn: Research and Development Division (1)

Commander
Air Material Command
Wright-Patterson Air Force Base
Dayton, Ohio
Attn: MCREX-B (1)
        Structures Division (1)

Commander
U.S. Air Force Institute of Technology
Wright-Patterson Air Force Base
Dayton, Ohio
Attn: Chief, Applied Mechanics Group (1)

Director of Intelligence
Headquarters, U.S. Air Force
Washington 25, D. C.
Attn: P.V. Branch (Air Targets Division) (1)

Commander
Air Force Office of Scientific Research
Washington 25, D. C.
Attn: Mechanics Division (1)

U.S. Atomic Energy Commission
Washington 25, D. C.
Attn: Director of Research (2)

Director
National Bureau of Standards
Washington 25, D. C.
Attn: Division of Mechanics (1)
        Engineering Mechanics Section (1)
        Aircraft Structures (1)

Commandant
U.S. Coast Guard
1300 E. Street, N. W.
Washington 25, D. C. (1)
Attn: Chief, Testing and Development Division

U.S. Maritime Administration
General Administration Office Building
441 G Street, N. W.
Washington 25, D. C.
Attn: Chief, Division of Preliminary Design

National Aeronautics and Space Administration
1512 H Street, N. W.
Washington 25, D. C.
Attn: Loads and Structures Division (2)

Director
National Aeronautics and Space Administration
Langley Research Center
Langley Field, Virginia
Attn: Structures Division (2)

Director, Forest Products Laboratory (1)
Madison, Wisconsin

Federal Aviation Agency
Department of Commerce
Washington 25, D. C.
Attn: Chief, Aircraft Engineering Division (1)
        Chief, Airframe and Equipment Branch (1)

National Sciences Foundation
1520 H Street, N. W.
Washington, D. C.
Attn: Engineering Sci. Div. (1)

National Academy of Sciences
2101 Constitution Avenue
Washington 25, D. C.
Attn: Technical Director, Committee on (1)
        Ships' Structural Design
        Executive Secretary, Committee on (1)
        Undersea Warfare

General Dynamics Corporation
Electric Boat Division (1)
Groton, Connecticut

Ingalls Shipbuilding Corporation
Pascagoula, Mississippi (1)

Professor Lynn S. Beedle
Fritz Engineering Laboratory (1)
Lehigh University
Bethlehem, Pennsylvania

Professor R. L. Bisplinghoff
Department of Aeronautical Engineering (1)
Massachusetts Institute of Technology
Cambridge 39, Massachusetts

Professor H. H. Bleich
Department of Civil Engineering (1)
Columbia University
New York 27, New York

Professor B. A. Boley
Department of Civil Engineering (1)
Columbia University
New York 27, New York

Dr. John F. Brahtz
Department of Engineering (1)
University of California
Los Angeles, California

Dr. D. O. Brush
Structures Department 53-13 (1)
Lockheed Aircraft Corporation
Missile Systems Division
Sunnyvale, California

Professor D. Budiansky
Department of Mechanical Engineering (1)
School of Applied Sciences
Harvard University
Cambridge 38, Massachusetts

Professor G. F. Carrier
Pierce Hall (1)
Harvard University
Cambridge 38, Massachusetts

Professor Herbert Deresiewicz
Department of Civil Engineering (1)
Columbia University
632 W. 125th Street
New York 27, New York

Professor R. A. Di Taranto
Department of Mechanical Engineering (1)
Drexel Institute
32nd and Chestnut Streets
Philadelphia, Pennsylvania

Professor D. C. Drucker, Chairman (1)
Division of Engineering
Brown University
Providence 12, Rhode Island

Professor A. C. Eringen
Department of Aeronautics Engineering (1)
Purdue University
Lafayette, Indiana

Professor J. Ericksen
Mechanical Engineering Department (1)
Johns Hopkins University
Baltimore 18, Maryland

Professor W. Flügge
Department of Mechanical Engineering (1)
Stanford University
Stanford, California

Mr. Martin Goland, President
Southwest Research Institute (1)
8500 Culebra Road
San Antonio 6, Texas

Professor J. N. Goodier
Department of Mechanical Engineering (1)
Stanford University
Stanford, California

Professor L. E. Goodman
Engineering Experiment Station (1)
University of Minnesota
Minneapolis, Minnesota

Professor M. Hetényi
The Technological Institute (1)
Northwestern University
Evanston, Illinois

Professor P. G. Hodge
Department of Mechanics (1)
Illinois Institute of Technology
Chicago 16, Illinois

Professor N. J. Hoff, Head
Division of Aeronautical Engineering (1)
Stanford University
Stanford, California

Professor Bruce G. Johnston
University of Michigan (1)
Ann Arbor, Michigan

Professor W. H. Hoppmann, II
Department of Mechanics (1)
Rensselaer Polytechnic Institute
Troy, New York

Professor J. Kempner
Department of Aeronautical Engineering (1)
and Applied Mechanics
Polytechnic Institute of Brooklyn
333 Jay Street
Brooklyn 1, New York

Professor H. L. Langhaar (1)
Department of Theoretical and Applied Mechanics
University of Illinois
Urbana, Illinois

Professor B. J. Lazan, Director
Engineering Experiment Station (1)
University of Minnesota
Minneapolis 14, Minnesota

Professor E. H. Lee
Division of Applied Mathematics (1)
Brown University
Providence 12, Rhode Island

Mr. S. Levy
General Electric Research Laboratory (1)
3198 Chestnut Street
Philadelphia, Pennsylvania

Professor Paul Lieber
Geology Department (1)
University of California
Berkeley 4, California

Newport News Shipbuilding and Dry Dock Co. (1)
Newport News, Virginia